Unveiling the Intrinsic Properties of Pyramidal Neurons In the Hippocampal Area Under AD

Devika Menon[1]

Received August 19, 2025
Accepted April 19, 2026
Electronic access June 30, 2026

Alzheimer's Disease (AD) is a devastating neurodegenerative condition that primarily affects the elderly. It is characterized by memory impairment, synaptic dysfunction, and progressive cognitive decline. The hippocampus, pivotal to memory and learning processes, is a central locus of pathological alterations in AD. Examining the intrinsic properties of neurons affected by this disease provides insight into the cellular processes underlying hippocampal dysfunction. While much research has examined synaptic dysfunction in AD, far fewer studies have explored how changes in the intrinsic properties of individual neurons may influence disease progression, despite their potential as early biomarkers and therapeutic targets. The findings presented here are based on original experimental data collected by the Daou Lab and analyzed in this study. The aim is to identify key differences in intrinsic properties, such as amplitude, threshold, and spike width, of pyramidal neurons in the hippocampus of mice with AD compared with controls. Whole-cell current-clamp recordings were obtained from hippocampal slices of both AD model mice and control mice to quantify these electrophysiological parameters. Analysis of these recordings revealed that neurons from AD-affected mice were significantly more excitable than those from controls, and several intrinsic properties were altered in the AD case. These findings suggest that further pharmacological investigations should be applied to identify the specific ion channels responsible for the altered excitability observed in AD neurons, potentially offering new targets for therapeutic intervention.

Keywords: Alzheimer's disease, hippocampus, pyramidal neurons, intrinsic excitability, spike amplitude, spike threshold, spike width, afterhyperpolarization (AHP), ion channel dynamics, electrophysiology, neurodegeneration

Introduction

Alzheimer's disease (AD) is a progressive neurodegenerative disorder that advances through distinct stages, with late-stage disease causing severe cognitive and physical decline, including loss of movement, communication, and awareness, and most commonly affecting individuals over 65, particularly women who are at higher risk due to longer lifespans [1,2].

AD is a growing global health concern, with prevalence increasing as the world's population ages. Currently, over 55 million people worldwide live with dementia, projected to rise to 139 million by 2050. AD accounts for 60–70% of cases, with nearly 10 million new diagnoses annually [3,4]. As the most common cause of dementia, AD contributes significantly to disability and dependency among older adults worldwide [5]. This rising prevalence underscores the urgent need to understand the disease's underlying mechanisms to develop effective treatments and interventions. The increasing prevalence of AD poses major challenges to healthcare systems and societies, highlighting the urgent need for improved understanding of its underlying mechanisms [4,6].

First, we discuss the pathology of AD (neurofibrillary tangles and amyloid-beta plaques), the concept of intrinsic plasticity, and the impact AD has on the hippocampus. Next, this study assesses differences in intrinsic properties of hippocampal pyramidal neurons in mice with and without AD. We assessed several key electrophysiological parameters, including spike threshold, which is the minimum membrane voltage needed to trigger an action potential; time to peak afterhyperpolarization (ttAHP), the time it takes for the neuron's membrane potential to reach its maximum negative value following an action potential; afterhyperpolarization (AHP), the period when the membrane potential becomes more negative than its resting state and helps regulate neuron firing; and spike width and amplitude, which describe the duration and size of the action potential, respectively. When assessing the pathology of AD, attention typically centers on synaptic connections, the communication between neurons, and how these are affected by neurofibrillary tangles and amyloid plaques. However, far less consideration is given to how the intrinsic properties of neurons themselves contribute to disease progression. These intrinsic properties encompass the internal mechanisms that govern neuronal excitability and signalling. By studying dif-

[1] *University of Toronto Schools, Ontario, Canada*

ferences in these intrinsic properties, we aim to better understand changes in fundamental cellular processes caused by AD within the hippocampus and provide insight into cellular mechanisms that may precede or accompany synaptic dysfunction.

Pathology of AD

Two of the most well-known biomarkers for AD are neurofibrillary tangles and amyloid-beta plaques. Neurofibrillary tangles consist of abnormal accumulations of abnormally phosphorylated microtubule protein tau within the perikaryal cytoplasm of pyramidal neurons [8]. The plaques consist of a peptide known as beta-amyloid, surrounded by abnormally configured neuronal processes or neurites [9].

Neurofibrillary tangles (NFTs) are composed of abnormal fibrils about 10 nm in diameter, occurring in pairs and bound in a helical structure [10]. They can have many different protein components associated with it, namely, ubiquitin, cholinesterase and beta-amyloid 4 [11]. However, the most important element is the tau protein, whose abnormal phosphorylation leads to these tangles [8]. Tau proteins regulate the assembly of microtubules, playing an integral role in neuronal development and axonal growth [10]. The phosphorylation and dephosphorylation of tau are maintained by a group of tau phosphates and microtubule-associated kinases [12]. In certain pathological conditions, the downregulation of these phosphates causes hyperphosphorylation of tau, resulting in insoluble double helicase filaments [13]. These filaments clump to form protein complexes, creating Neurofibrillary tangles (Figure 1). The tau proteins in AD lose their usual abilities to bind and stabilize microtubules in the axon [14]. These structures lead to the eventual depredation of neurons and survive even after the death of affected neurons. After neuronal death, they are released extracellularly and interact with astrocytes and microglia [15]. Areas affected by neurofibrillary tangles include the layer II neurons of the entorhinal cortex, the CA1 and subicular regions of the hippocampus, the amygdala, the dorsal raphae and the nucleus basalis of Meynert [16].

Another critical pathological lesion of AD is senile or neuritic plaques, otherwise known as amyloid plaques [18]. These plaques are extracellular accumulations of βA4, a peptide derived from the abnormal processing of amyloid precursor protein (APP) [19]. APP is a membrane protein in the endoplasmic reticulum and is transported to the Golgi complex to be cleaved by 3 secretases α, β, or γ [20]. Most notably, β-

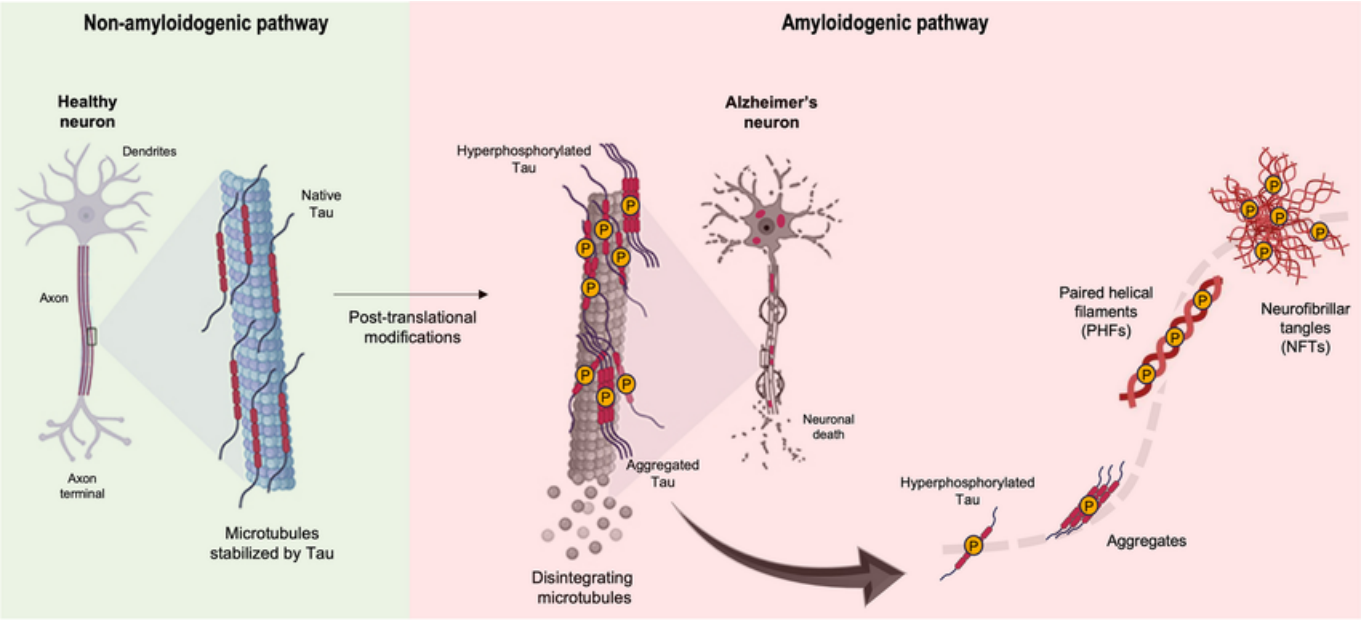

Fig. 1 Visual Depiction of Tau Pathology and Neurofibrillary Tangle Formation in AD. This figure illustrates the progression from healthy tau function to neurofibrillary tangles (NFT) formation in AD. In normal neurons (left, non-amyloidogenic pathway), tau proteins stabilize axonal microtubules, maintaining neuronal structure and function. However, in AD (right, amyloidogenic pathway), tau undergoes abnormal post-translational modifications, particularly hyperphosphorylation. This disrupts its microtubule-stabilizing role, causing tau to dissociate and aggregate. These aggregates form paired helical filaments (PHFs), which accumulate into intracellular neurofibrillary tangles. NFTs contribute to neuronal dysfunction, microtubule disintegration, and ultimately cell death. The figure aligns with key pathological features discussed in AD, emphasizing tau's transformation from a structural protein into a toxic aggregate that persists even after neuronal degeneration [7].

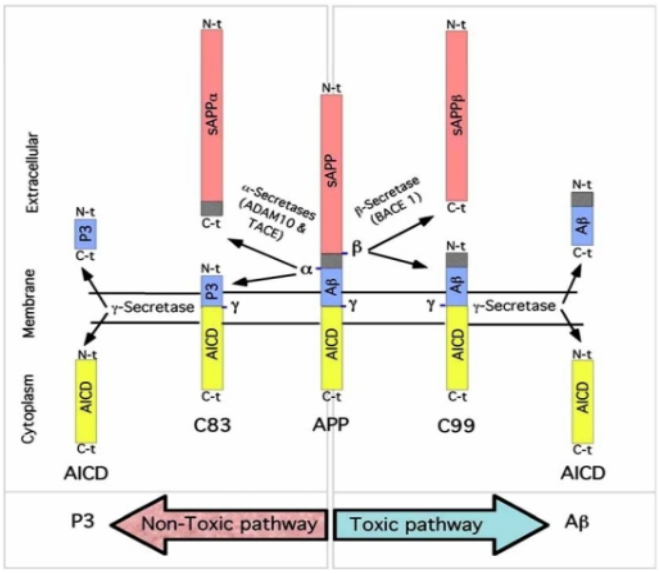

Fig. 2 Visual Depiction of APP Processing Pathways and Aβ Production in Alzheimer's Disease Pathology. This schematic illustrates the proteolytic processing of amyloid precursor protein (APP) through two distinct pathways: the non-toxic (non-amyloidogenic) and toxic (amyloidogenic) pathways, both crucial to Alzheimer's disease (AD) pathology. In the non-toxic pathway, APP is cleaved by α-secretase (ADAM10/TACE), producing soluble APP alpha (sAPPα) and preventing the formation of amyloid-beta (Aβ) peptides. Conversely, in the toxic pathway, β-secretase (BACE1) initiates cleavage, followed by γ-secretase, leading to the generation of Aβ peptides which aggregate extracellularly to form amyloid plaques, a hallmark of AD. The figure also shows the cleavage fragments p3 and Aβ, with the latter contributing to neurotoxic amyloid plaques. This dual-pathway processing emphasizes how altered proteolysis of APP contributes to AD pathology by fostering the accumulation of β-amyloid plaques, thereby disrupting neuronal function and promoting neurodegeneration [17].

secretase cleaves the amino terminal while γ-secretase cleaves the carboxy-terminal, releasing βA4 (Figure 2) [21]. Diffused plaques are the initial deposition of βA4 in the cerebral cortex, lacking dystrophic neurites and are commonly associated with non-cognitive dysfunction [18]. Neuritic plaques have a central βA4 core and are surrounded by dystrophic neurites, they are pathognomonic of AD and are linked to cognitive decline [18]. Together these mechanisms ultimately disrupt synaptic function, trigger neuroinflammatory responses and contribute to neuronal death [9].

Intrinsic Plasticity

Amyloid plaques and Tau tangles are widely recognized as the primary pathological markers of AD, playing a critical role in disrupting normal neuronal function. Inflammation, as well as the progressive loss of synapses, forms the crux of neurological damage seen in AD [22]. However, crucial factors that have been overlooked are how the intrinsic features and changes of neurons affect this disease. These intrinsic properties (IPs) are critical because they determine how neurons respond to inputs, regulate firing patterns, and maintain network stability [23]. Changes in intrinsic excitability can alter information processing and disrupt signal propagation, even without synaptic modifications. In AD, such alterations may contribute to network dysfunction by creating states of excessive or reduced excitability, which can impair learning and memory [24]. Investigating these intrinsic changes is therefore important, as it provides insight into cellular-level mechanisms of the disease and may reveal targets for interventions beyond synaptic pathways.

Intrinsic changes are distinct from synaptic changes. While synaptic changes involve alterations at the synapse, intrinsic plasticity refers to activity-dependent modifications in a neuron's own electrophysiological properties [25]. These changes are mediated by ion channels and affect processes such as synaptic integration, subthreshold signal propagation, spike generation, and meta-plasticity [26]. By adjusting these intrinsic properties, neurons can regulate their excitability and responsiveness independently of synaptic modifications.

A neuron's ability to generate an action potential based on a stimulus is regulated by the number, type, and distribution of its voltage- and calcium-gated ion channels [27].

Furthermore, intrinsic plasticity is related to homeostatic regulation of neuronal firing. For example, depriving the neocortical or hippocampal neurons of electrical or synaptic stimulation for an extended period increased neuronal excitability, contrary to the results of synaptic plasticity [28]. Conversely, increasing neuronal input above the basal level was seen to decrease neuronal excitability. The changes and regulation of intrinsic excitability (IE) are attributed to the modification of ion channels in the neuron [29].

The Hippocampus and AD

Structure of the Hippocampus

The hippocampus, a key structure for memory and decision-making, is particularly vulnerable in Alzheimer's disease, where neuronal loss and synaptic dysfunction contribute to the characteristic memory deficits (refer to Figure 3 for the anatomical overview) [31,32].

Function and Impact of AD of the Hippocampus

The hippocampus is involved in various cognitive functions, particularly memory, learning, and spatial navigation [33]. It

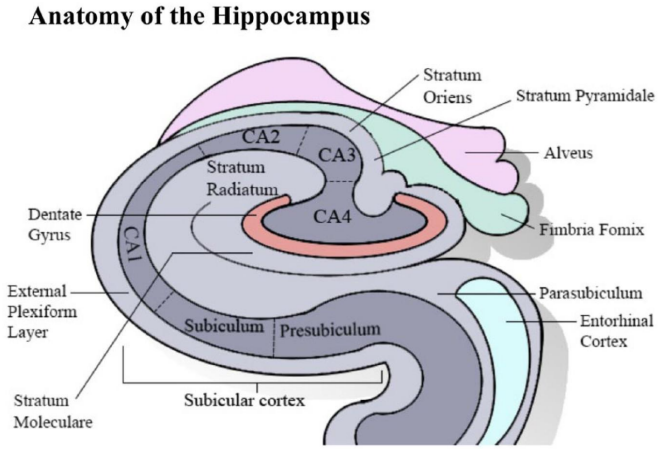

Fig. 3 Anatomical Subregions and Layers of the Hippocampus. This figure illustrates the anatomy of the hippocampus, highlighting its major subfields including Cornu Ammonis regions CA1 through CA4, the dentate gyrus, subiculum, presubiculum, and surrounding structures such as the entorhinal cortex and fimbria-fornix. Key cellular layers such as the stratum oriens, stratum pyramidale, stratum radiatum, stratum lacunosum-moleculare, alveus, and external plexiform layer are identified, reflecting the layered organization essential for hippocampal function. This anatomical organization underpins critical cognitive processes like memory consolidation and spatial navigation, which are notably disrupted in Alzheimer's disease through neurodegeneration and synaptic loss primarily targeting regions like CA1 and the dentate gyrus[30].

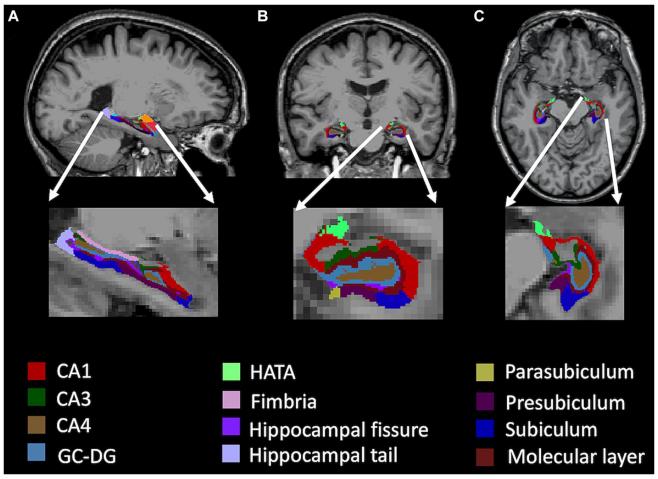

Fig. 4 MRI-Based Segmentation of Human Hippocampal Subfields in Three Planes Relevant to AD. Segmented MRI views (sagittal, coronal, axial) of the human hippocampus highlighting major subfields, including CA1–CA4, dentate gyrus (GC-DG), subiculum, and associated structures. These regions play distinct roles in memory and learning, with CA1 critical for episodic encoding and the dentate gyrus for adult neurogenesis. In Alzheimer's disease, pathology begins with tau accumulation in CA1 and spreads to other subfields, while amyloid-β deposits first appear in the entorhinal cortex and progress into the hippocampus. Subfield-specific atrophy shown here reflects patterns of neurodegeneration underlying memory impairment and hippocampo-cortical dissociation.anatomical organization underpins critical cognitive processes like memory consolidation and spatial navigation, which are notably disrupted in Alzheimer's disease through neurodegeneration and synaptic loss primarily targeting regions like CA1 and the dentate gyrus[39].

is one of the few regions in the brain where neurogenesis—mainly in the dentate gyrus—continues into adulthood[34]. Though initially thought to have little impact, this ongoing neurogenesis is now understood to contribute to memory processing, as new neurons integrate into existing neural networks and assist in memory consolidation[35]. The hippocampus plays a crucial role in encoding and retrieving spatial, episodic, and semantic memories and communicates with the neocortex—particularly during memory encoding (hippocampus) and retrieval (neocortex)[36]. Memory is processed through two primary pathways: the polysynaptic and direct intra-hippocampal pathways. The polysynaptic pathway involves afferent connections from the parietal, temporal, and occipital lobes via the entorhinal cortex, traveling through the dentate gyrus, CA3, CA1, and subiculum, before reaching the anterior thalamus and cingulate cortex[37]. The direct pathway carries inputs from the temporal association cortex through entorhinal areas directly to CA1, impacting episodic and spatial memory[36]. The hippocampus also influences decision-making and memory consolidation, particularly in transforming short-term into long-term memory, which supports future decision-making[38].

Specific to AD, neuronal loss and gliosis in the hippocampal region is a prevalent pathological feature[18]. Early dysfunction and synaptic loss that primarily affects excitatory transmission in the hippocampus and cerebral cortex, are key contributors to memory loss in AD[40]. Vulnerable regions include glutamatergic neurons in the entorhinal cortex and pyramidal neurons in CA1[41]. Histopathologically, AD is characterized by neurofibrillary tangles (NFTs) composed of hyperphosphorylated tau protein, first appearing in the CA1 region before spreading to the subiculum, CA2, CA3, and dentate gyrus (DG)[18](Figure 4). Concurrently, amyloid-beta (Aβ) plaques accumulate in the entorhinal cortex and later invade the hippocampus, disrupting synaptic communication[18]. These degenerative changes are exacerbated by neuroinflammation, oxidative stress, and gliosis, resulting in hippocampal atrophy, reduced cortical connectivity, and cognitive dysfunction, as described by the "hippocampo-cortical dissociation" hypothesis[42]. Imaging studies show bilateral atrophy in hippocampal layers such as the stratum radiatum, stratum lacunosum, and subiculum's stratum pyramidale, all detectable through

MRI[43]. Disruptions in glutamatergic, serotonergic, and noradrenergic neurotransmitter systems correlate with neuronal loss. Experimental models also link tau and Aβ pathology with disrupted DG connectivity, paralleling the progressive degeneration observed in human AD[10]. Clinically, hippocampal damage manifests as memory deficits, including both anterograde and retrograde amnesia, with advanced AD stages marked by severe cognitive decline and confabulations[44].

Methods

This experiment focuses on extracting and comparing the intrinsic features of hippocampal pyramidal neurons in both Alzheimer's and Control groups. The data was provided by the Daou Lab.

Alzheimer's disease model mice used in the current study were generated using the APP transgenic mice (PDAPP), which causes robust amyloid-beta plaque deposition. Control animals, referred to as the "intact" group, were not genetically modified and served as the control. All the animals were maintained under controlled settings and manipulated in line with the animal research ethics guidelines. All the procedures were subject to approval by the University of Chicago Institutional Animal Care and Use Committee (IACUC).

Hippocampal tissue slices were prepared from the CA1 region of the hippocampus of a total of 11 adult male mice (5 control and 6 Alzheimer's disease model), with each animal contributing one neuron to the dataset. The CA1 subfield was targeted given its selective vulnerability to neurofibrillary tangle accumulation and synaptic loss in AD. There were 5 adult male control mice and 6 adult males with Alzheimer's disease, each contributing 1 neuron. All animals were bred and maintained under standard laboratory conditions at the University of Chicago and were randomly selected for experimentation. Only healthy, adult males were used to reduce variability due to developmental or hormonal differences. After deep anesthesia with isoflurane, animals were decapitated, and brains were rapidly removed and placed in ice-cold artificial cerebrospinal fluid (ACSF) containing (in mM): 119 NaCl, 2.5 KCl, 1.3 $MgCl_2$, 2.5 $CaCl_2$, 1.0 NaH_2PO_4, 26.2 $NaHCO_3$, and 22 glucose (pH 7.2–7.3; 285–295 mOsm), aerated with a 95% O_2 / 5% CO_2 gas mix. Slices were cut at 300–400 μm thickness using a vibratome and placed directly into an oxygenated ACSF-filled incubation chamber at 37°C. Slices were incubated at 37°C for at least 1 hour and then allowed to equilibrate to room temperature ($\sim$24–25°C) prior to recordings. Whole-cell current-clamp recordings were obtained using borosilicate glass pipettes with a resistance of 3-8 MΩ, filled with intracellular solution containing (in mM): 135 K-gluconate, 10 HEPES, 2 Mg-ATP, 0.3 Na-GTP, 0.2 EGTA, pH adjusted to 7.2–7.3 with KOH. Tight-seal recordings ($>$1 GΩ) were obtained, and neurons were allowed to dialyze for several minutes before stimulation. Series resistance (Rs) was monitored throughout each recording and compensated online when necessary. Cells were included in the analysis only if they met the following criteria: resting membrane potential ≤ -65 mV at baseline and stable throughout the recording, series resistance between 3.5–10 MΩ, and consistent spiking across the recording period. Input resistance was measured from small hyperpolarizing current steps (5-25 pA, 200–300 ms), and leak currents were monitored to ensure recording stability. All recordings were conducted blind to experimental group. Recordings were obtained under visual control using a Multiclamp 700B amplifier, and data were sampled at 50 kHz.

Pharmacological blockers were utilized to suppress synaptic input throughout electrophysiological recordings, thereby isolating intrinsic neuronal excitability from synaptic contributions. All drug treatments were administered via a gravity-fed perfusion system that facilitated continuous and accurate delivery to the tissue slices. Synaptic transmission was blocked in all standard recordings using NMDA, AMPA/kainate, $GABA_a$, and GABA+ receptor antagonists (CNQX, CPP, Gabazine, and CGP 35348), ensuring that the action potential properties measured reflect intrinsic excitability rather than network-driven activity. Additional voltage-gated channel blockers—including cadmium chloride, TEA, cesium chloride, and TTX—were applied selectively in mechanistic sub-experiments designed to isolate specific ionic conductances, and were not used during the standard action potential recordings reported here.

For the purposes of this paper, the primary coding language used to extract the features of the spikes is Python. Using Python allowed for leverage of the versatile and rich libraries that were available for scientific computing and data visualization. In addition, the Spyder software was used to run the code as well as curate graphs and visualizations for the given data.

For each detected spike, a local window around the peak was extracted to isolate individual action potential (AP) events. Within this window, three principal components of the AP were quantified: the threshold, defined as the first point where the membrane potential's rate of change (dV/dt) exceeded 0.5 mV per sample—equivalent to 25 mV/ms at the 50 kHz sampling rate—consistent with the derivative-based approach described in Daou and Margoliash (2020)[45]. Prior to computing dV/dt, voltage traces were smoothed using a Gaussian kernel with a standard deviation of 1 sample ($\sim$0.02 ms) to reduce high-frequency noise while preserving the rapid depolarization of genuine action potentials; the peak, corresponding to the maximum voltage within the spike; and the afterhyperpolarization (AHP), defined as the difference between the threshold and the minimum voltage following the peak within the same window. Spike amplitude was calculated as the difference between the peak and the threshold voltage

(Figure 5). The width of the spike was estimated as the duration over which the membrane potential exceeded half the spike amplitude. The time to peak and time to AHP were computed as the respective latencies from the threshold point. Spike frequency was calculated as the total number of spikes divided by the duration of the detected stimuli (in seconds), yielding a measure of firing rate in Hertz. For all pairwise comparisons between AD and control neurons, independent samples t-tests were performed using Python's SciPy library. A threshold of $p < 0.01$ was used to define statistical significance.

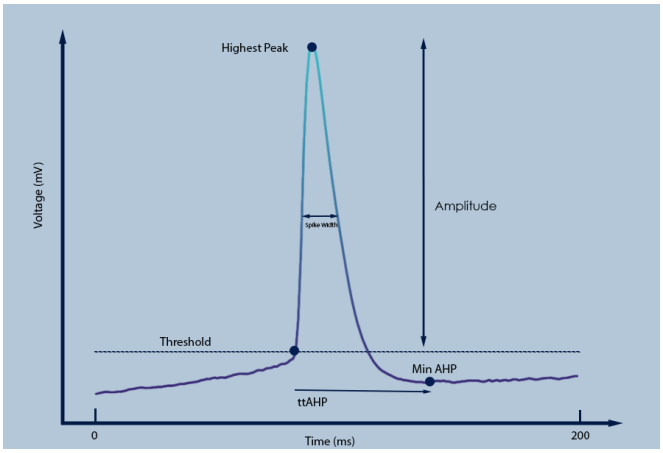

Fig. 5 Single Action Potential Isolated from Raw Neuronal Voltage Trace, Visualizing Firing Patterns of AD and Control Neurons A single spike was isolated from the raw voltage trace in the from the control neuron (N1) dataset by detecting peaks above the mean membrane potential. A 200-sample window (±100 samples) was extracted around the third spike to visualize one clean action potential. Illustrated, is the progression of a neuronal action potential. The labeled waveform highlights measurable parameters including spike **amplitude** (the voltage difference from resting potential to peak), **threshold** (the minimum depolarization required to trigger a spike), **AHP** (afterhyperpolarization, the hyperpolarized phase following the spike), **TTAHP** (time to afterhyperpolarization, the duration from spike onset to AHP peak), and **spike width** (the duration of the action potential at half-maximal amplitude).

Results

To investigate the IPs of hippocampal pyramidal neurons in Alzheimer's disease (AD) mouse model, we firstly visualized the spikes trains of their elicited membrane potential traces in response to current stimuli and compared them with quantitative metrics of spiking dynamics between AD and control groups. Representative traces revealed that AD neurons (Figure 6) exhibited a dramatically markedly increased elevated spike frequency, narrower spike widths, and lower peaks in comparison with control neurons (Figure 6).

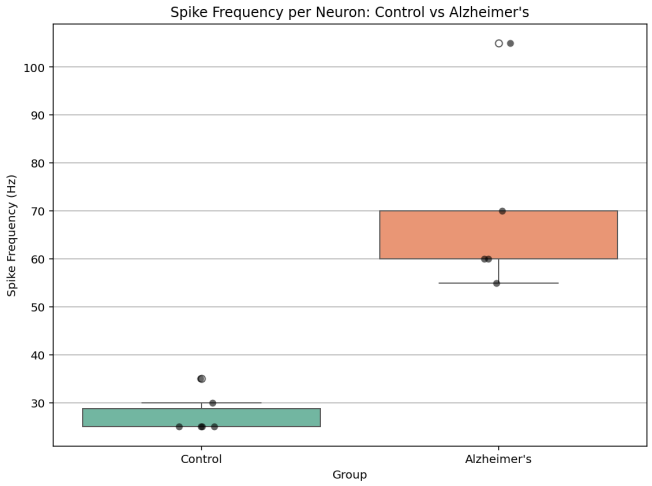

Fig. 6 Boxplot Representing the Firing Pattern Distribution between Alzheimer's and Control Neurons. The Boxplot illustrating the distribution of spike frequencies in control versus Alzheimer's neurons. Control neurons exhibit significantly lower and more consistent spike frequencies, typically around 25–35 Hz, indicating stable and regulated firing activity. In contrast, Alzheimer's neurons display markedly elevated and more variable spike frequencies (ranging from 55–105 Hz), reflecting increased neuronal excitability.

The spike amplitude of APs directly influences the strength of neuronal firing and the efficacy of subsequent synaptic transmission, while spike width and time to peak play crucial roles in determining the temporal precision of information encoding and the ability to sustain high-frequency firing. A detailed analysis of these features can thus provide important insights into the altered intrinsic properties of neurons in AD. With this consideration in mind, we quantified spike amplitude, spike width, and time to peak in both control and AD neurons, as illustrated in Figure 7. ($t = 11.63$), $p<0.01$).

Possible explanations as to what lower spike amplitudes could signify include reduced voltage-gated sodium channel availability or partial channel inactivation, which would limit the inward Na^+ current during the depolarization phase and thereby reduce peak voltage. Upregulation of potassium channel conductance could further truncate the amplitude by accelerating repolarization before the peak is reached. Furthermore, physiological changes to neurons such as synaptic loss and axonal degradation may result in weaker spike propagation and reduced signal strength. The changes seen in Figure 7 could represent the loss of functional homeostasis in the neural network, potentially contributing to cognitive deficits seen in AD.

The next feature measured was the spike threshold, which was seen to be significantly more depolarized in AD samples compared to controls ($t = -4.99$, $p<0.01$). Examining

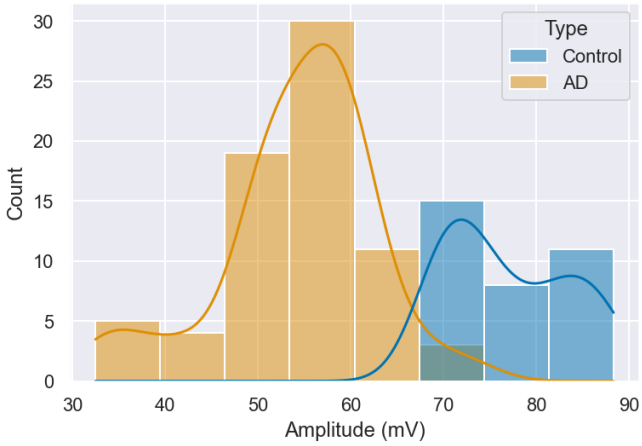

Fig. 7 Histogram Representing the Relationship Between Amplitudes of Control and AD groups. In this graph, control neurons display higher amplitudes, with a more uniform distribution, ranging from 65-87 mV and peaking around 69 mV. Conversely AD samples exhibited a broader range of spike amplitudes, ranging from 30-90 mV and peaking at 60 mV

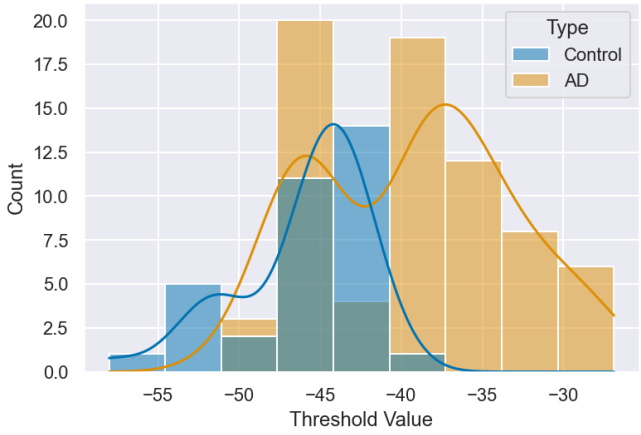

Fig. 8 Histogram Representing the Relationship Between Threshold Values of Control and AD groups. Control groups showed values ranging from -59 to -41 mV, peaking at around -44 mV. AD samples demonstrated threshold values in a broad range of -60 to -25 mV, peaking at around -46 and -38 mV.

the thresholds for each individual spike elicited in both control and AD pyramidal neurons showed significant changes among the two groups (Figure 8). Spike threshold is a critical determinant of IE and dictates the minimum voltage required to initiate an AP, it thereby influencing the neuron's responsiveness to incoming stimuli.

A spike's threshold is largely determined by voltage-gated sodium channels, which open to allow the influx of sodium ions during the initiation of an action potential. The increased depolarization of the neurons in the AD group could suggest reduced sensitivity of sodium channels or altered gating mechanisms. In particular, downregulation of Nav1.6—a sodium channel subtype highly expressed in hippocampal pyramidal neurons—or a depolarizing shift in its steady-state inactivation curve could reduce the number of available channels at rest, requiring greater depolarization to reach threshold. With a higher spike threshold, neurons are less responsive to excitatory input and may fail to fire altogether during low-frequency stimulation.

The AHP values for the action potentials were significantly higher in AD neurons compared to controls (Figure 9) ($t = -7.18$, $p < 0.01$). The AHP that follows each spike is an important determinant of intrinsic excitability. It sets the refractory window and modifies the pattern and accuracy of recurrent firing. The amplitude of the AHP and the time it takes to reach its peak (time to AHP peak) determine how effectively a neuron can manage incoming signals and how quickly it can get back to firing. Thus, changes in these properties could have great effects on how neuronal networks perform.

AHP is primarily mediated by calcium-activated potassium channels, particularly small-conductance (SK) and large-conductance (BK) channels, and contributes to the resetting of the membrane potential following each action potential. In this study, the AHP amplitude was significantly higher in AD neurons compared to controls. Importantly, this larger measured AHP amplitude does not contradict the observed increase in spike frequency. In AD, downregulation of SK channel expression and activity is well established, which functionally reduces the inhibitory SK-mediated K^+ current that normally suppresses repetitive firing. When SK channel currents are diminished, the inhibitory brake on neuronal firing is weakened, allowing neurons to fire more rapidly despite the presence of a larger AHP—a dissociation that has been documented in models of hippocampal hyperexcitability. The enlarged AHP amplitude observed here may therefore reflect a compensatory upregulation of other potassium conductances, or altered calcium-activated channel kinetics, rather than a net increase in inhibitory tone. Critically, it is also important to note that a central feature of AD neurotoxicity is the disruption of intracellular calcium homeostasis. Elevated intracellular Ca^{2+} levels resulting from dysregulated endoplasmic reticulum (ER) Ca^{2+} release and impaired buffering can directly activate calcium-sensitive potassium channels including SK and BK channels, thereby modifying AHP amplitude and contributing to altered firing patterns. Resting membrane potential was not significantly different between groups, indicating that the increased excitability is primarily driven by altered ion channel dynamics rather than a shift in baseline membrane state.

No significant difference was found in time to peak AHP

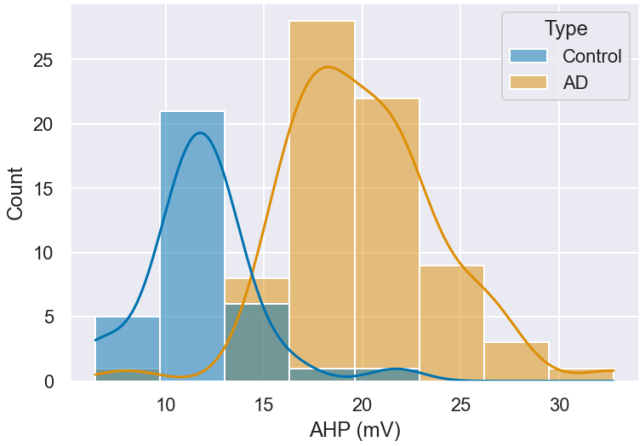

Fig. 9 Histogram Representing the Relationship Between AHP Values of Control and AD groups. Control neurons exhibited lower AHP values, ranging from 4 – 13 mV and peaking at around 10 mV. Conversely, the AD neurons constituted a broader range of -5 to 34 mV, peaking at around 19 mV.

between control and AD samples (Figure 10) (t = -0.75, p = 0.46). This suggests that the timing of the AHP remains largely consistent between the two groups. The preservation of time-to-peak AHP suggests that while the amplitude of potassium channel-mediated currents may be altered in AD neurons, the kinetics of channel activation and deactivation remain largely intact. This dissociation between amplitude and timing may indicate that the number or conductance of active channels is affected, rather than the fundamental gating properties of the channels themselves.

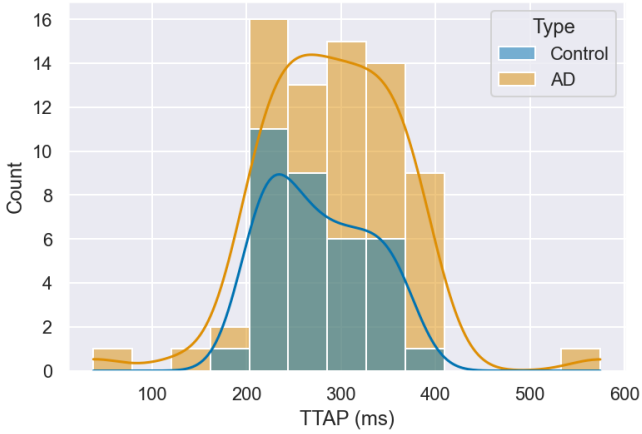

Fig. 10 Histogram Representing the Relationship Between TTAHP Values of Control and AD groups. Both groups exhibit relatively overlapping distributions. AD neurons seem to have a broader variety of TTAHP values ranging from 50 to 400 ms.

Finally, the spike widths in AD neurons tended to be narrower, suggesting that the duration of the action potential was reduced compared to the control group (Figure 11). This could imply that the depolarization phase of the action potential is shorter, possibly reflecting faster repolarization and altered ion channel dynamics. The narrowing of spike width may reflect enhanced potassium channel conductance and/or reduced sodium channel availability, both of which would accelerate repolarization. Upregulation of voltage-gated K^+ channels such as Kv3 or Kv4.2 could drive faster repolarization, while reduced Nav channel density would limit the duration of the inward Na^+ current sustaining the depolarization plateau. Statistically, the differences between the two groups did not reach the pre-defined significance threshold (t = 2.26, p = 0.03), and this trend warrants further investigation with larger sample sizes.

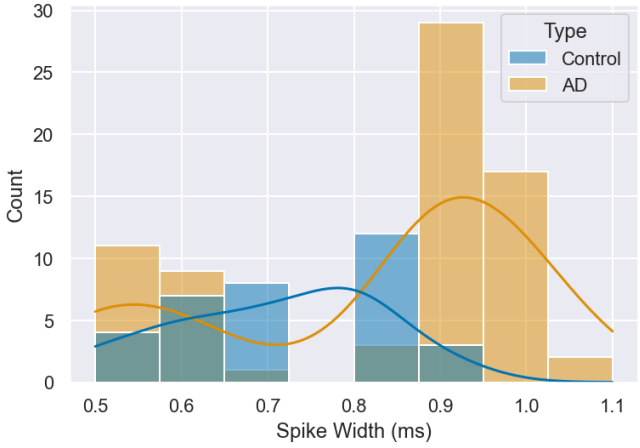

Fig. 11 Histogram Representing the Relationship Between Spike Width of Control and AD groups. The AD group has a broader distribution of values ranging from 0.1 to 1.05 ms, peaking at about 0.29 ms. Whereas the control group ranges from 0.1 to 0.2, peaking at around 0.1 ms.

Conclusion

Our results reveal robust alterations in intrinsic properties of hippocampal pyramidal neurons in the AD mouse model compared to healthy controls, extending current understanding of AD-related hippocampal dysfunction. Specifically, we observed consistent changes across several features, including spike amplitude, spike width, time to peak, AHP amplitude, and time to AHP peak. These findings support our original hypothesis that hippocampal neurons in AD undergo intrinsic excitability changes that may reflect early biophysical correlates of cognitive dysfunction.

The increased spike frequency in AD neurons suggests enhanced intrinsic excitability, likely driven by altered ion channel function. Downregulation of SK channels reduces the afterhyperpolarization-mediated inhibitory brake on repetitive firing, while downregulation of Kv1 channels shortens interspike intervals and weakens spike-frequency adaptation. Possible downregulation of Kv3 channels, which support fast spiking, may further contribute to this phenotype. In parallel, reduced Nav1.6 availability or a depolarizing shift in its inactivation curve may lower the spike threshold and accelerate depolarization, facilitating earlier firing despite reduced peak amplitude. Together, these intrinsic mechanisms likely underlie the heightened excitability observed here, and this increased excitability is consistent with previous studies linking AD to excitotoxicity in the hippocampus[46]. It is important to note that while the recordings in this study were performed under synaptic blockade—isolating intrinsic excitability from network-driven input—in the intact AD brain, synaptic changes would act in concert with the intrinsic alterations described here. In particular, AD-related downregulation of inhibitory $GABA_a$ currents and upregulation of excitatory AMPA receptor activity would further promote neuronal hyperexcitability beyond what is observed from intrinsic mechanisms alone. The results presented here therefore represent a lower bound on the degree of excitability change in the living AD brain.

A further interpretive framework worth considering is that of homeostatic plasticity. The observed changes in intrinsic properties—including higher spike threshold, larger AHP amplitude, and reduced spike amplitude—may not represent purely pathological degeneration, but could in part reflect compensatory responses by which neurons attempt to counteract an initial state of hyperexcitability driven by amyloid-beta toxicity, elevated intracellular calcium, and disrupted synaptic inhibition. Under this homeostatic view, neurons upregulate inhibitory conductances (such as calcium-activated K^+ channels driving the AHP) to dampen excessive firing, while the downstream SK channel downregulation ultimately overcomes this compensation, resulting in net hyperexcitability. This framework is consistent with the concept of intrinsic homeostatic plasticity, whereby activity-dependent modifications of ion channel expression maintain neuronal firing within a functional range—a mechanism that is known to be disrupted in neurodegenerative disease contexts.

One important interpretive framework for these findings is homeostatic plasticity. The observed changes—including elevated AHP amplitude, higher spike threshold, and reduced spike amplitude—may not represent purely pathological deterioration, but rather a compensatory response by which neurons attempt to counteract an initial state of hyperexcitability driven by amyloid-beta toxicity, impaired calcium buffering, and disrupted inhibitory tone. Under this framework, the neuron upregulates inhibitory conductances in an attempt to restore firing to a physiological set point. However, if SK channel downregulation simultaneously reduces the effectiveness of the AHP as an inhibitory brake, the net result is paradoxical: compensatory changes fail to suppress firing, and neurons remain hyperexcitable despite the presence of a larger AHP. This interplay between Hebbian and homeostatic plasticity mechanisms highlights the complexity of excitability changes in AD and underscores the need for mechanistic follow-up studies to disentangle adaptive from maladaptive alterations.

These findings highlight the importance of intrinsic neuronal properties in the pathophysiology of AD, emphasizing that alterations in the ionic mechanisms governing action potential generation and repolarization can lead to impaired neuronal communication, network dysfunction, and ultimately cognitive decline. In doing so, our work contributes to filling a gap in the literature by quantitatively linking specific biophysical changes in hippocampal neurons to potential early drivers of AD pathology, providing a cellular-level perspective that complements existing synaptic and molecular studies. Understanding these changes in neuronal excitability provides crucial insights into the underlying cellular mechanisms of AD, with potential implications for the development of targeted therapeutic strategies aimed at restoring normal neuronal function and mitigating the cognitive impairments associated with the disease. For example, future research could employ pharmacological modulation of specific potassium and sodium channels in vivo to determine whether normalizing excitability can rescue memory performance in AD models or use high-resolution imaging to track how these excitability changes progress during disease stages.

One limitation of this study is the relatively modest sample size, which may affect the statistical power and generalizability of certain findings.

In conclusion, the observed alterations in neuronal excitability may represent an early and targetable component of AD pathology, suggesting that therapies aimed at stabilizing intrinsic firing properties could complement approaches focused on reducing amyloid or tau pathology. By advancing our understanding of how the disease alters the fundamental electrical behavior of hippocampal neurons, this study underscores the importance of integrating electrophysiological biomarkers into both basic and translational AD research, helping to build a clearer connection between cellular-level changes and the progression of cognitive symptoms in Alzheimer's disease.

References

1 B. Reisberg, S. H. Ferris, M. J. Leon and T. Crook, Functional staging of dementia of the Alzheimer type. Annals of the New York Academy of Sciences, vol. 435, pp. 481–483, 1984. https://doi.org/10.1111/j.1749-6632.1984.tb13859.x.

2 M. T. Ferretti, M. F. Iulita, E. Cavedo, P. A. Chiesa, A. S. Dimech, A. S. Chadha and H. Hampel, Sex and gender differences in Alzheimer's disease: current challenges and implications for clinical practice. European Journal of Neurology, vol. 27, pp. 928–943, 2020. https://doi.org/10.1111/ene.14174.

3 Alzheimer's Disease International, World Alzheimer Report 2019: Attitudes to dementia. ADI, London, 2019.

4 World Health Organization, Dementia. World Health Organization Fact Sheets, 2021. https://www.who.int/news-room/fact-sheets/detail/dementia.

5 M. Prince, G. C. Ali, M. Guerchet, A. M. Prina, E. Albanese and Y. T. Wu, Recent global trends in the prevalence and incidence of dementia, and survival with dementia. Alzheimer's Research & Therapy, vol. 8, p. 23, 2016. https://doi.org/10.1186/s13195-016-0188-8.

6 GBD 2019 Dementia Forecasting Collaborators, Estimation of the global prevalence of dementia in 2019 and forecasted trends through 2050: an analysis for the Global Burden of Disease Study 2019. The Lancet Public Health, vol. 7, pp. 105–125, 2022. https://doi.org/10.1016/S2468-2667(21)00249-8.

7 Z. L. Almeida, D. C. Vaz and R. M. Brito, Morphological and molecular profiling of amyloid-β species in Alzheimer's pathogenesis. Molecular Neurobiology, vol. 62, pp. 4391–4419, 2024. https://doi.org/10.1007/s12035-024-04543-4.

8 K. Iqbal and I. Grundke-Iqbal, Alzheimer neurofibrillary degeneration: significance, etiopathogenesis, therapeutics and prevention. Journal of Cellular and Molecular Medicine, vol. 12, pp. 38–55, 2008. https://doi.org/10.1111/j.1582-4934.2008.00225.x.

9 R. H. Takahashi, T. Nagao and G. K. Gouras, Plaque formation and the intraneuronal accumulation of β-amyloid in Alzheimer's disease. Pathology International, vol. 67, pp. 185–193, 2017. https://doi.org/10.1111/pin.12520.

10 T. F. Gendron and L. Petrucelli, The role of tau in neurodegeneration. Molecular Neurodegeneration, vol. 4, p. 13, 2009. https://doi.org/10.1186/1750-1326-4-13.

11 D. P. Perl, Neuropathology of Alzheimer's disease. Mount Sinai Journal of Medicine: A Journal of Translational and Personalized Medicine, vol. 77, pp. 32–42, 2010. https://doi.org/10.1002/msj.20157.

12 Y. Xia, S. Prokop and B. I. Giasson, Don't phos over tau: recent developments in clinical biomarkers and therapies targeting tau phosphorylation in Alzheimer's disease and other tauopathies. Molecular Neurodegeneration, vol. 16, p. 46, 2021. https://doi.org/10.1186/s13024-021-00460-5.

13 A. Schneider, J. Biernat, M. Von Bergen, E. Mandelkow and E. M. Mandelkow, Phosphorylation that detaches tau protein from microtubules (Ser262, Ser214) also protects it against aggregation into Alzheimer paired helical filaments. Biochemistry, vol. 38, pp. 3549–3558, 1999. https://doi.org/10.1021/bi981874p.

14 Y. Chen and Y. Yu, Tau and neuroinflammation in Alzheimer's disease: interplay mechanisms and clinical translation. Journal of Neuroinflammation, vol. 20, p. 165, 2023. https://doi.org/10.1186/s12974-023-02853-3.

15 H. S. Kwon and S. Koh, Neuroinflammation in neurodegenerative disorders: the roles of microglia and astrocytes. Translational Neurodegeneration, vol. 9, p. 30, 2020. https://doi.org/10.1186/s40035-020-00221-2.

16 C. M. Moloney, V. J. Lowe and M. E. Murray, Visualization of neurofibrillary tangle maturity in Alzheimer's disease: a clinicopathologic perspective for biomarker research. Alzheimer's & Dementia, vol. 17, pp. 1554–1574, 2021. https://doi.org/10.1002/alz.12321.

17 Creative Diagnostics, App processing and plaque formation. Creative Diagnostics Technical Resources. https://www.creative-diagnostics.com/app-processing-and-plaque-formation.htm.

18 M. A. DeTure and D. W. Dickson, The neuropathological diagnosis of Alzheimer's disease. Molecular Neurodegeneration, vol. 14, p. 32, 2019. https://doi.org/10.1186/s13024-019-0333-5.

19 M. M. Rahman and C. Lendel, Extracellular protein components of amyloid plaques and their roles in Alzheimer's disease pathology. Molecular Neurodegeneration, vol. 16, p. 40, 2021. https://doi.org/10.1186/s13024-021-00465-0.

20 Y. W. Zhang, R. Thompson, H. Zhang and H. Xu, App processing in Alzheimer's disease. Molecular Brain, vol. 4, p. 3, 2011. https://doi.org/10.1186/1756-6606-4-3.

21 S. L. Cole and R. Vassar, The Alzheimer's disease beta-secretase enzyme, BACE1. Molecular Neurodegeneration, vol. 2, p. 22, 2007. https://doi.org/10.1186/1750-1326-2-22.

22 M. Colom-Cadena, T. Spires-Jones, H. Zetterberg, K. Blennow, A. Caggiano, S. T. DeKosky, J. E. Harrison, L. S. Schneider, P. Scheltens, W. De Haan, M. Grundman, C. H. Van Dyck, N. J. Izzo and S. M. Catalano, The clinical promise of biomarkers of synapse damage or loss in Alzheimer's disease. Alzheimer's Research & Therapy, vol. 12, p. 21, 2020. https://doi.org/10.1186/s13195-020-00588-4.

23 J. Gjorgjieva, R. A. Mease, W. J. Moody and A. L. Fairhall, Intrinsic neuronal properties switch the mode of information transmission in networks. PLoS Computational Biology, vol. 10, p. e1003962, 2014. https://doi.org/10.1371/journal.pcbi.1003962.

24 T. Guo, D. Zhang, Y. Zeng, T. Y. Huang, H. Xu and Y. Zhao, Molecular and cellular mechanisms underlying the pathogenesis of Alzheimer's disease. Molecular Neurodegeneration, vol. 15, p. 40, 2020. https://doi.org/10.1186/s13024-020-00391-7.

25 G. Daoudal and D. Debanne, Long-term plasticity of intrinsic excitability: learning rules and mechanisms. Learning & Memory, vol. 10, pp. 456–465, 2003. https://doi.org/10.1101/lm.64103.

26 A. x. Patel and D. Burdakov, Mechanisms of gain control by voltage-gated channels in intrinsically-firing neurons. PLOS ONE, vol. 10, p. e0115431, 2015. https://doi.org/10.1371/journal.pone.0115431.

27 A. Daou and D. Margoliash, Intrinsic plasticity and birdsong learning. Neurobiology of Learning and Memory, vol. 180, p. 107407, 2021. https://doi.org/10.1016/j.nlm.2021.107407.

28 J. Echegoyen, A. Neu, K. D. Graber and I. Soltesz, Homeostatic plasticity studied using in vivo hippocampal activity-blockade: synaptic scaling, intrinsic plasticity and age-dependence. PLOS ONE, vol. 2, p. e700, 2007. https://doi.org/10.1371/journal.pone.0000700.

29 T. O'Leary, M. C. W. Van Rossum and D. J. A. Wyllie, Homeostasis of intrinsic excitability in hippocampal neurones: dynamics and mechanism of the response to chronic depolarization. The Journal of Physiology, vol. 588, pp. 157–170, 2010. https://doi.org/10.1113/jphysiol.2009.181024.

30 C. C. Pang, C. Kiecker, J. T. O'Brien, W. Noble and R. C. Chang, Ammon's horn 2 (CA2) of the hippocampus: a long-known region with a new potential role in neurodegeneration. The Neuroscientist, vol. 25, pp. 167–180, 2018. https://doi.org/10.1177/1073858418778747.

31 M. A. Meyer, The hippocampus. Neurologic Disease, Springer, Cham, pp. 127–141, 2016. https://doi.org/10.1007/978-3-319-39581-4_6.

32 L. A. Fogwe, V. Reddy and F. B. Mesfin, Neuroanatomy, hippocampus. StatPearls [Internet], Treasure Island (FL): StatPearls Publishing, 2023. https://www.ncbi.nlm.nih.gov/books/NBK482171.

33 H. Eichenbaum, The role of the hippocampus in navigation is memory. Journal of Neurophysiology, vol. 117, pp. 1785–1796, 2017. https://doi.org/10.1152/jn.00005.2017.

34 R. Knoth, I. Singec, M. Ditter, G. Pantazis, P. Capetian, R. P. Meyer, V. Horvat, B. Volk and G. Kempermann, Murine features of neurogenesis in the human hippocampus across the lifespan from 0 to 100 years. PLOS ONE, vol. 5, p. e8809, 2010. https://doi.org/10.1371/journal.pone.0008809.

35 A. Wu and J. Zhang, Neuroinflammation, memory, and depression:

new approaches to hippocampal neurogenesis. Journal of Neuroinflammation, vol. 20, p. 191, 2023. https://doi.org/10.1186/s12974-023-02964-x.

36 K. T. Sumadevi, The hippocampus: anatomy, function and clinical correlation. Sri Lanka Anatomy Journal, vol. 8, pp. 6–20, 2024. https://doi.org/10.4038/slaj.v8i1.220.

37 S. Ohara, S. Sato, K. Tsutsui, M. P. Witter and T. Iijima, Organization of multisynaptic inputs to the dorsal and ventral dentate gyrus: retrograde trans-synaptic tracing with rabies virus vector in the rat. PLOS ONE, vol. 8, p. e78928, 2013. https://doi.org/10.1371/journal.pone.0078928.

38 L. R. Squire, L. Genzel, J. T. Wixted and R. G. Morris, Memory consolidation. Cold Spring Harbor Perspectives in Biology, vol. 7, p. a021766, 2015. https://doi.org/10.1101/cshperspect.a021766.

39 Y. Xiao, Y. Hu and K. Huang, Atrophy of hippocampal subfields relates to memory decline during the pathological progression of Alzheimer's disease. Frontiers in Aging Neuroscience, vol. 15, p. 1287122, 2023. https://doi.org/10.3389/fnagi.2023.1287122.

40 L. Crews and E. Masliah, Molecular mechanisms of neurodegeneration in Alzheimer's disease. Human Molecular Genetics, vol. 19, pp. 12–20, 2010. https://doi.org/10.1093/hmg/ddq160.

41 G. W. Van Hoesen, B. T. Hyman and A. R. Damasio, Entorhinal cortex pathology in Alzheimer's disease. Hippocampus, vol. 1, pp. 1–8, 1991. https://doi.org/10.1002/hipo.450010102.

42 B. T. Hyman, G. W. Van Hoesen, A. R. Damasio and C. L. Barnes, Alzheimer's disease: cell-specific pathology isolates the hippocampal formation. Science, vol. 225, pp. 1168–1170, 1984. https://doi.org/10.1126/science.6474172.

43 E. Frankó, O. Joly and Alzheimer's Disease Neuroimaging Initiative, Evaluating Alzheimer's disease progression using rate of regional hippocampal atrophy. PLOS ONE, vol. 8, p. e71354, 2013. https://doi.org/10.1371/journal.pone.0071354.

44 W. B. Scoville and B. Milner, Loss of recent memory after bilateral hippocampal lesions. The Journal of Neurology, Neurosurgery, and Psychiatry, vol. 20, pp. 11–21, 1957. https://doi.org/10.1136/jnnp.20.1.11.

45 A. Daou and D. Margoliash, Intrinsic neuronal properties represent song and error in zebra finch vocal learning. Nature Communications, vol. 11, p. 952, 2020. https://doi.org/10.1038/s41467-020-14738-7.

46 Q. Deng, X. Yu, Y. Qin, S. Chen, J. Zhao and H. Zhang, Microglia and astrocytes in Alzheimer's disease: significance and summary of recent advances. Aging and Disease, vol. 14, p. 12, 2023. https://doi.org/10.14336/ad.2023.0907.